NJC

(1,6)Pyrenophanes containing crown ether moieties as fluorescence sensors for metal and ammonium ions. Formation of sandwich, dumbbell, and pseudorotaxane complexes

Journal:	*New Journal of Chemistry*
Manuscript ID	NJ-ART-09-2022-004790.R1
Article Type:	Paper
Date Submitted by the Author:	08-Dec-2022
Complete List of Authors:	Maeda, Hajime; Kanazawa University, Division of Material Chemistry, Graduate School of Natural Science and Technology Saito, Genki; Kanazawa University, Division of Material Chemistry, Graduate School of Natural Science and Technology Furuyama, Taniyuki; Kanazawa University, Division of Material Chemistry, Graduate School of Natural Science and Technology; Japan Science and Technology Agency Segi, Masahito; Kanazawa University, Division of Material Chemistry, Graduate School of Natural Science and Technology

SCHOLARONE™
Manuscripts

ARTICLE

(1,6)Pyrenophanes containing crown ether moieties as fluorescence sensors for metal and ammonium ions. Formation of sandwich, dumbbell, and pseudorotaxane complexes

Received 00th January 20xx,
Accepted 00th January 20xx

DOI: 10.1039/x0xx00000x

Hajime Maeda,*[a] Genki Saito,[a] Taniyuki Furuyama[a,b] and Masahito Segi[a, ‡]

(1,6)Pyrenophanes **1** and **2** in which 1,6-positions of pyrene are bridged with respective tri- and tetra-ethylene glycol chains were synthesized. Addition of $Ba(ClO_4)_2$ to a 10^{-5} M CH_2Cl_2 : CH_3CN = 1 : 1 solution of **1** reduced the intramolecular excimer emission with a maximum at 480 nm and increased the monomer emission around 370–400 nm. In contrast, addition of $Ba(ClO_4)_2$ to the solution of **2** shifted the intramolecular excimer emission to shorter wavelengths. Addition of n-$Bu_2NH_2^+PF_6^-$ to the solutions of **1** and **2** both decreased the intramolecular excimer emission and increased the monomer emission. Based on the results of these fluorescence changes, Job's plots, and NMR titration, it is concluded that **1** forms a 1:1 sandwich-type complex with Ba^{2+}, **2** forms a 1:2 dumbbell-type complex with Ba^{2+}, and both **1** and **2** form pseudorotaxanes with n-$Bu_2NH_2^+$. It was also found that when the pyrenophanes **1** and **2** were mixed with tetracyanoethylene (TCNE) in CH_2Cl_2, charge-transfer (CT) complexes were formed, that exhibited absorption maxima at 740 and 744 nm, respectively.

Introduction

Pyrene is known to emit monomer fluorescence from a single excited singlet molecule and excimer fluorescence from an excited singlet dimer in solution.[1-3] Due to this dual fluorescence character, in addition, high photostability and high fluorescence quantum yield, many pyrene-based fluorescent compounds have been synthesized and investigated.[4-19] Among them, pyrenophanes, in which two pyrenes are linked at two or more sites, have attracted interest from the viewpoints of their structures (planar/bending), fluorescence properties (monomer/excimer emission), and guest inclusion abilities.[3,20] Grouping the pyrenophanes by their bridging positions, there are (1,6),[21-31] (2,7),[22,23,31-39] (1,3),[40-45] (1,8),[21,46] (7,1,3)[47-49] pyrenophanes. Particularly, (1,6)pyrenophane skeleton has been utilized for development of compounds that exhibit only intramolecular excimer emissions,[22,27] inclusion ability of aromatic compounds,[24,25] circularly polarized luminescence (CPL),[31] and mechanoresponsive luminescence and liquid-crystalline behaviour.[28,30]

On the other hand, many studies have been conducted on compounds that link pyrene with crown ethers or oligoethylene glycols as fluorescence sensors that recognize metal ions.[50-92] They can be classified into three types, turn-ON[50-58] and turn-OFF types[59-63] depending on photoinduced electron transfer and heavy atom effect, and monomer/excimer emission switching type[64-84] depending on the spatial distance between two pyrenes.

In earlier efforts, we have synthesized (1,3)[45] and (1,8)pyrenophanes[46] in which the 1,3- or 1,8-positions of pyrene are linked with oligoethylene glycol chains, and have shown that they work as effective fluorescence sensor molecules that can switch the *anti*- and *syn*-structures that emit respective monomer and intramolecular excimer fluorescence depending on solvent polarity and temperature. In this study, we synthesized (1,6)pyrenophanes in which the 1,6-positions of pyrene are linked with oligoethylene glycol chains, and investigated the absorption/fluorescence properties when metal ions, ammonium ions, and electron-deficient compounds were added.

Results and discussion

(1,6)pyrenophanes **1**, **2** and reference compounds **3**-**6** were synthesized by using the routes shown in Scheme 1. Bromination of pyrene **7** with two equivalents of Br_2 gave 1,6-dibromopyrene **8**, that was treated with *t*-BuLi followed by DMF to give 1,6-diformylpyrene **9**. Reduction of **9** with $NaBH_4$ gave diol **10**, whose iodination with NaI/Me_3SiCl produced 1,6-bis(iodomethyl)pyrene **11**. Pyrenophane **1** was synthesized by Williamson ether synthesis using **11** and triethylene glycol in 3% yield. Similarly, pyrenophane **2** was synthesized in 4% yield by reacting **11** with tetraethylene glycol. As its by-product, the 1:1 adduct **3** was formed in 4% yield. On the other hand, when **11** was reacted with diethylene glycol, the corresponding

[a] Division of Material Chemistry, Graduate School of Natural Science and Technology, Kanazawa University, Kakuma-machi, Kanazawa, Ishikawa 920-1192, Japan.
[b] Japan Science and Technology Agency (JST)-PRESTO, 4-1-8 Honcho, Kawaguchi, Saitama 332-0012, Japan.
† Electronic Supplementary Information (ESI) available: [details of any supplementary information available should be included here]. See DOI: 10.1039/x0xx00000x
‡ Present address: Ishikawa Study Center, The Open University of Japan, 7-1 Ohgigaoka, Nonoichi, Ishikawa 921-8812, Japan.

pyrenophane was not obtained, however, ring-opened compounds **12** and **13** were obtained in 13% and 5% yields, respectively. The reaction of **11** with pentaethylene glycol was slow, and 3 days reflux gave the corresponding pyrenophane in 1% yield, however, its isolation was unsuccessful. 1,6-Bis(methoxymethyl)pyrene **4** was prepared by the reaction of diol **10** with MeI. Bis(pyrenylmethyl) oligoethylene glycols **5** and **6** were synthesized from pyrene in four steps according to literature.[77] The structures of the synthesized pyrenophanes **1**, **2** and reference compounds **3**-**6** were determined by ^{1}H NMR, ^{13}C NMR, IR and mass spectra.

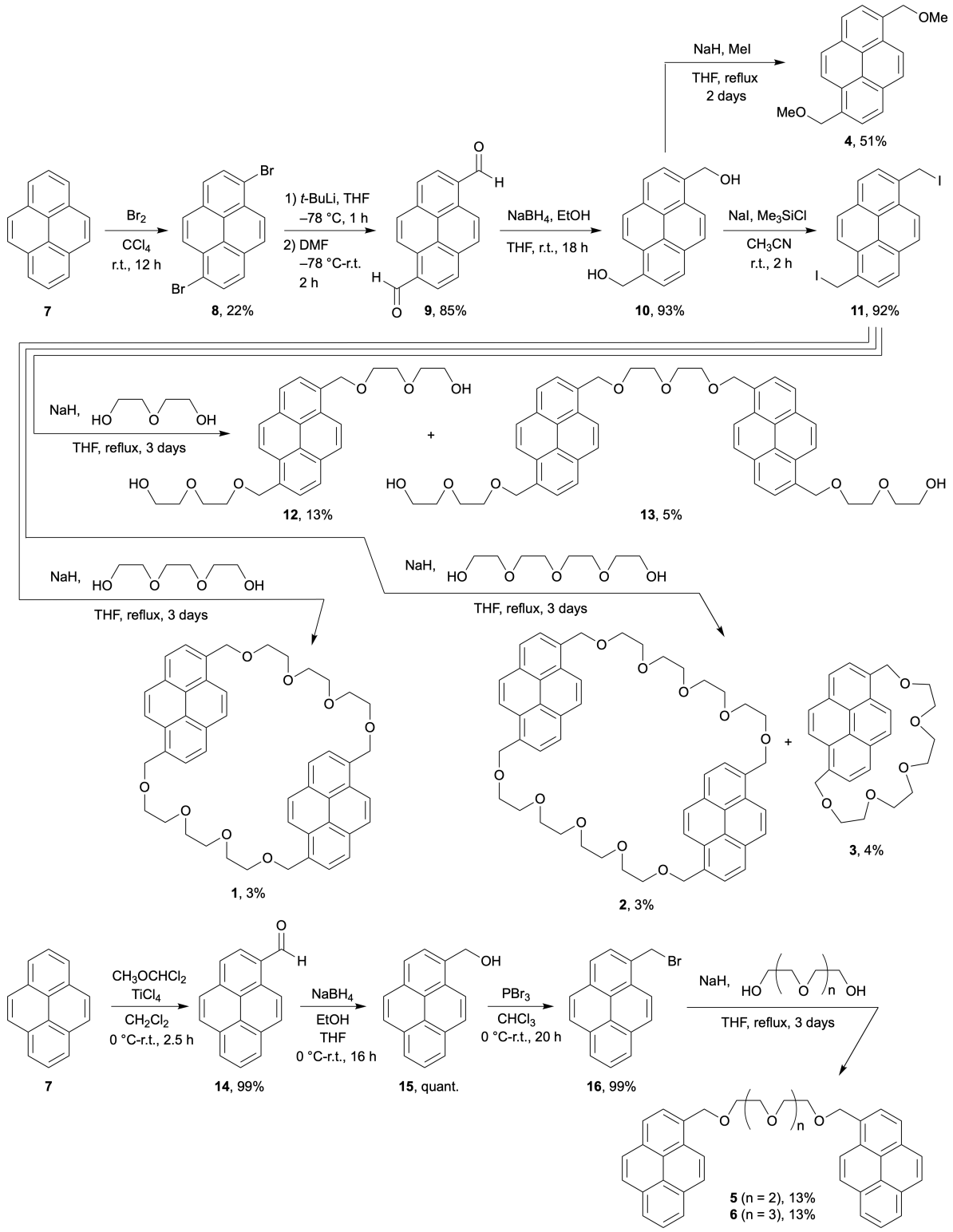

Scheme 1 Synthesis of (1,6)pyrenophanes linked by oligoethylene glycols **1** and **2** and reference compounds **3**-**6**.

This journal is © The Royal Society of Chemistry 20xx

Please do not adjust margins

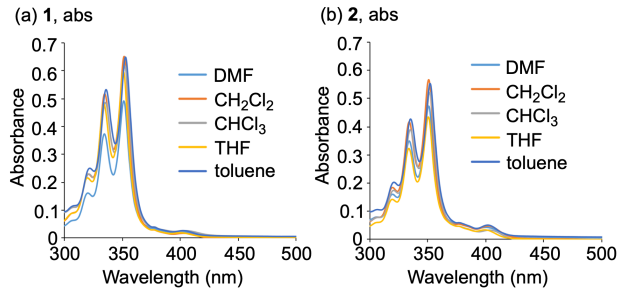

Fig. 1 UV-vis absorption spectra of (a) **1** and (b) **2** (1.0×10^{-5} M).

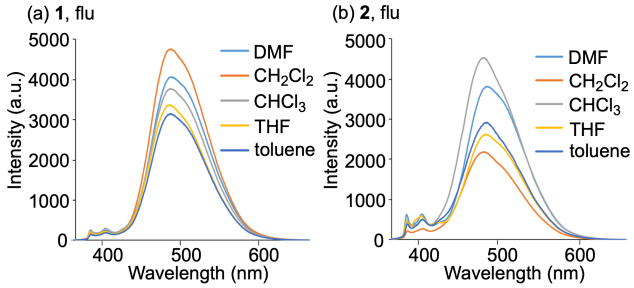

Fig. 2 Fluorescence spectra of (a) **1** (1.0×10^{-5} M, λ_{ex} = 350.5-352.5 nm) and (b) **2** (1.0×10^{-5} M, λ_{ex} = 350.5-352 nm).

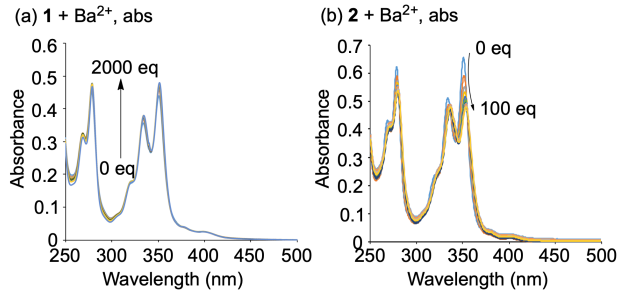

Fig. 3 UV-vis absorption spectra of (a) **1** and (b) **2** (1.0×10^{-5} M in CH_2Cl_2 : CH_3CN = 1 : 1) upon addition of $Ba(ClO_4)_2$ ((a) 0-2000 equiv, (b) 0-100 equiv).

(1,6)Pyrenophanes have C_{2h} and D_2 symmetrical atrop isomers depending on the orientation of the pyrene ring.[20,21,31] Variable temperature ^{1}H NMR spectra of **1**, **2** was measured in $CDCl_3$ (–60 to 60 °C) and toluene-d_8 (–80 to 100 °C), however, no coalescence was observed in this temperature range, indicating that the pyrene rings are fully rotated (Fig. S1, S2). UV-vis absorption spectra of pyrenophanes **1** and **2** were investigated in DMF, CH_2Cl_2, $CHCl_3$, THF, and toluene (Fig. 1). Both **1** and **2** showed absorption bands based on the π-π* transition of pyrene (λ_{max} =350-353 (**1**), 350-352 (**2**) nm), and no particular solvent dependence was confirmed. The fluorescence of **1** and **2** was measured in the same five solvents, showing strong intramolecular excimer emission (λ_{max} = 480-482 nm (**1**, **2**)) along with weak monomer emission (λ_{max} = 379-380, 398-400 (**1**, **2**)), especially no significant difference in wavelength due to the solvent was observed (Fig. 2).

UV-vis absorption spectra were taken when $Ba(ClO_4)_2$ was added to 1.0×10^{-5} M in CH_2Cl_2 : CH_3CN = 1 : 1 solutions of compounds **1** and **2** (Fig. 3). Although no significant change was observed, addition of Ba^{2+} to the solution of **1** resulted in a slight longer wavelength shift and an increase in absorbance. On the other hand, addition of Ba^{2+} to the solution of **2** resulted in a longer wavelength shift and a significant decrease in absorbance.

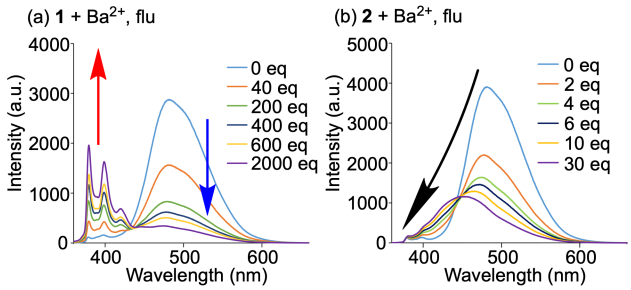

Fig. 4 Fluorescence spectra of (a) **1** and (b) **2** (1.0×10^{-5} M in CH_2Cl_2 : CH_3CN = 1 : 1) upon addition of $Ba(ClO_4)_2$ ((a) 0-2000 equiv, (b) 0-30 equiv), λ_{ex} = 350 nm.

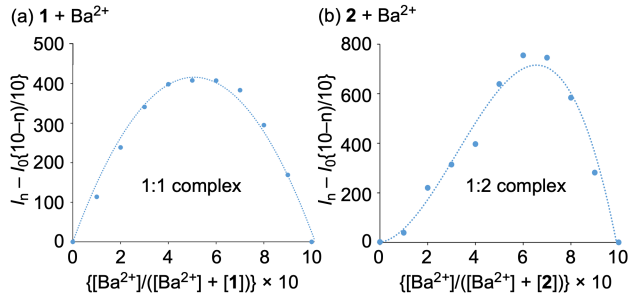

Fig. 5 Job's plot for complexation of (a) **1** and (b) **2** with Ba^{2+} obtained from change of fluorescence at 480 nm in CH_2Cl_2 : CH_3CN = 1 : 1, [**1** or **2**] + [$Ba(ClO_4)_2$] = 1.0×10^{-5} M.

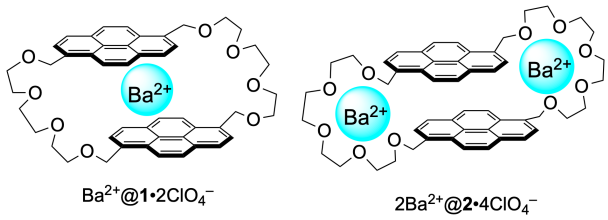

Fig. 6 Proposed structures of sandwich and dumbbell complexes.

Up to 2000 equivalents of $Ba(ClO_4)_2$ was added to a 1.0×10^{-5} M CH_2Cl_2 : CH_3CN = 1 : 1 solution of pyrenophane **1**, and changes in the fluorescence spectrum were investigated (Fig. 4a). As a result, intramolecular excimer emission decreased and monomer emission increased. In contrast, in compound **2**, the maximum of intramolecular excimer emission shifts from 481 nm to 447 nm continuously with the addition of as few as 30 equivalents of Ba^{2+} (Fig. 4b). In other words, it was found that **1** and **2** showed completely different fluorescence behaviors against addition of Ba^{2+}.

Please do not adjust margins

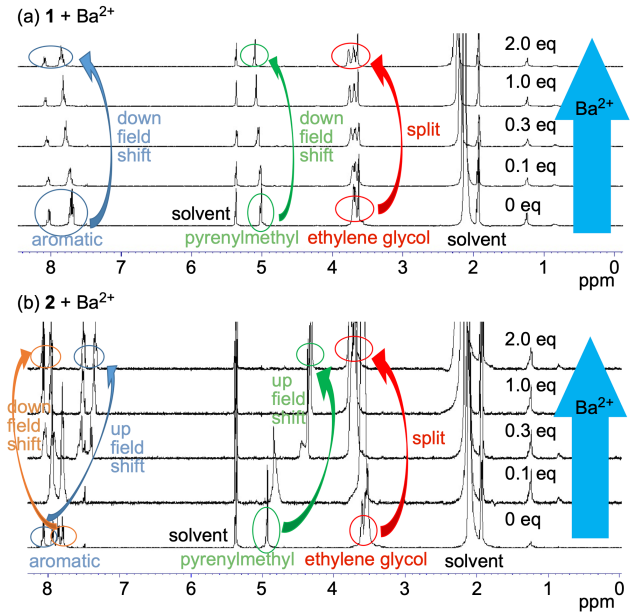

Fig. 7 500 MHz ^{1}H NMR spectra of (a) **1** and (b) **2** upon addition of $Ba(ClO_4)_2$ in CD_2Cl_2 : CD_3CN = 1 : 1, $[\mathbf{1}]_0 = [\mathbf{2}]_0 = 3.0 \times 10^{-3}$ M.

Job's plot was performed based on the change in the fluorescence spectrum (Fig. 5). The results suggested that **1** forms a 1:1 complex with Ba^{2+} and **2** forms a 1:2 complex. Based on the fluorescence spectroscopic change and the results of Job's plot, it was assumed that **1** forms a sandwich type 1:1 complex with Ba^{2+}, and **2** formed a dumbbell-type 1:2 complex with Ba^{2+} (Fig. 6). The complexation constant was calculated from the change in the fluorescence spectrum, and it was found that **1** forms a complex with Ba^{2+} in one-step equilibrium (K = 2.26×10^3 M^{-1}), while **2** forms a complex with Ba^{2+} in two-step equilibrium ($K_1 = 1.95 \times 10^5$, $K_2 = 2.76 \times 10^4$ M^{-1}).

It may be difficult to imagine the complex unrelated to the oxygen atoms. However, we would like to propose the formation of pyrene-Ba^{2+}-pyrene sandwich complex **5**. As pyrene-metal-pyrene complexes, V, Nb, Ti complexes have been isolated.[93] In addition, pyrene-metal cation-π interactions are also confirmed in systems of unsubstituted pyrene with Ag^+ [94] and alkali metal ions,[95] ionic liquid linked pyrene with K^+ and Cs^+,[96] and azacrown ether linked pyrene with Li^+.[51]

Changes when Ba^{2+} was added to CD_2Cl_2 : CD_3CN = 1 : 1 solutions of **1** and **2** were monitored by ^{1}H NMR spectra (Fig. 7, full data is Fig. S3). By increasing the equivalents of Ba^{2+} added to the solution of **1**, a significant downfield shift of the resonance of the pyrene ring of **1** was observed, while the symmetry on the pyrene ring was maintained. A slight downfield shift of the resonance at the pyrenylmethyl hydrogens of **1** was observed. With the addition of Ba^{2+}, splitting of the resonance of ethylene glycol chain of **1** was observed, but the chemical shift of the resonance was almost unchanged. On the other hand, in the NMR titration experiment of **2**, it was found that two 2H resonances in the pyrene region shifted to the low magnetic field, and the remaining two 2H resonances shifted to the high magnetic field. The symmetry on the pyrene ring also maintained. The ethylene glycol chain of **2** was split and shifted downfield unlike **1**. The hydrogens at the pyrenylmethyl position of **2** underwent a large upfield shift. The downfield shift of the pyrene region of **1** is thought to be due to the reduction of the electron density in the pyrene region due to Ba^{2+} coordination. The change in the pyrene region of **2** might be a consequence of the fact that the pyrene rings approach each other while being twisted, and complexation with Ba^{2+} causes four hydrogens to enter the shielded region of another pyrene and the remaining four hydrogens to enter the deshielded region of the other pyrene. The ethylene glycol chain of **1** did not change its electronic state much by the addition of Ba^{2+}, however, the ethylene glycol chain of **2** became electron-deficient by the addition of Ba^{2+}. The pyrenylmethyl hydrogens of **1** became slightly electron-deficient by the addition of Ba^{2+}, while those of **2** came to a position that greatly suffer the ring current effect of another pyrene by the addition of Ba^{2+}. Thus, these NMR spectral changes also support the formation of a sandwich-type structure of **1** and a dumbbell-type structure of **2**.

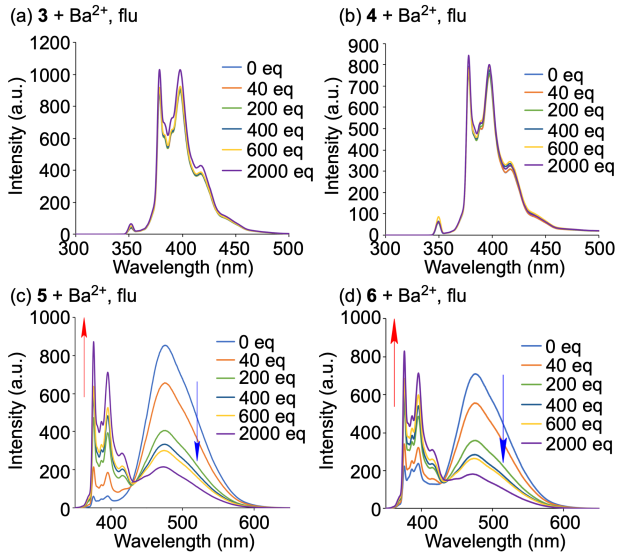

Fig. 8 Fluorescence spectra of (a) **3**, (b) **4**, (c) **5**, and (d) **6** (1.0×10^{-5} M in CH_2Cl_2 : CH_3CN = 1 : 1) upon addition of $Ba(ClO_4)_2$ (0-2000 equiv), λ_{ex} = (a) 351, (b) 350, (c)(d) 343 nm.

This journal is © The Royal Society of Chemistry 20xx

Please do not adjust margins

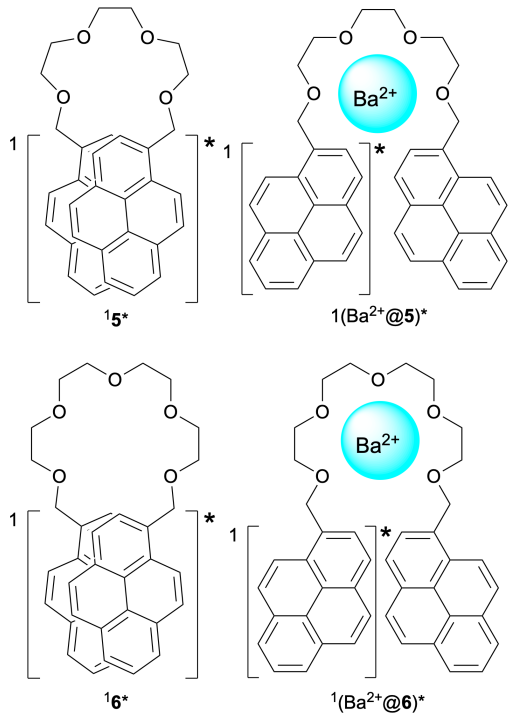

Fig. 9 Proposed excited state structures of **5** and **6** for the explanation of fluorescence spectral change upon addition of Ba^{2+}.

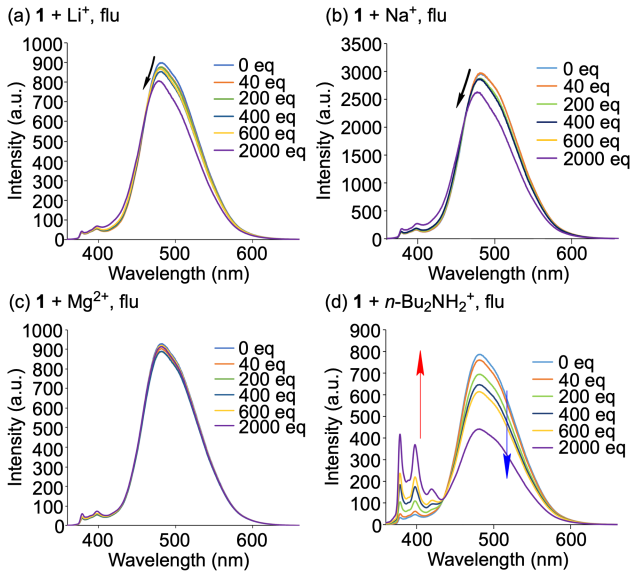

Fig. 10 Fluorescence spectra of **1** (1.0×10^{-5} M in CH_2Cl_2 : CH_3CN = 1 : 1) upon addition of (a) $LiClO_4$ (0-2000 equiv), (b) $NaClO_4$ (0-2000 equiv), (c) $Mg(ClO_4)_2$ (0-2000 equiv), and (d) n-$Bu_2NH_2^+PF_6^-$ (0-2000 equiv), λ_{ex} = (a)-(c) 351, (d) 350 nm.

Next, the change in fluorescence spectrum when $Ba(ClO_4)_2$ was added to each of reference compounds **3**-**6** was examined under the same conditions (Fig. 8). Compounds **3** and **4** showed only monomer fluorescence in the absence of metal ions, and the addition of 2000 equivalents of Ba^{2+} hardly changed the fluorescence spectra. In contrast, compounds **5** and **6** exhibit intramolecular excimer emission in the absence of metal ions, however, when Ba^{2+} was added, the intramolecular excimer fluorescence of both **5** and **6** decreased and monomer fluorescence increased. Using this change in fluorescence spectra, the complexation constants of **5** and **6** with Ba^{2+} were calculated to be $K = 9.49 \times 10^2$ M^{-1} (**5**), 8.13×10^2 M^{-1} (**6**), which are smaller values than those of pyrenophanes **1** and **2**. Compounds **5** and **6** exhibit intramolecular excimer emission in the absence of metal ions because their oligoethylene glycol chains are free to move (Fig. 9). When Ba^{2+} interacts with the oligoethylene glycol chains of **5** and **6** to form 1:1 complexes, the molecular motion is suppressed and the two pyrenes are no longer spatially close to each other.

When Li^+, Na^+, Mg^{2+}, and n-$Bu_2NH_2^+$ ions were added to the solution of **1**, the absorption spectra hardly changed (Fig. S4). In the fluorescence spectra (Fig. 10), when Li^+ and Na^+ were added to the solution of **1**, the intramolecular excimer emission was slightly shifted to the shorter wavelengths (λ_{max} = 479 (Li^+), 477 nm (Na^+)), however, when Mg^{2+} was added, there was almost no change in fluorescence wavelength (λ_{max} = 482 nm). When n-$Bu_2NH_2^+$ was added to the solution of **1**, the intramolecular excimer emission decreased and the monomer emission increased.

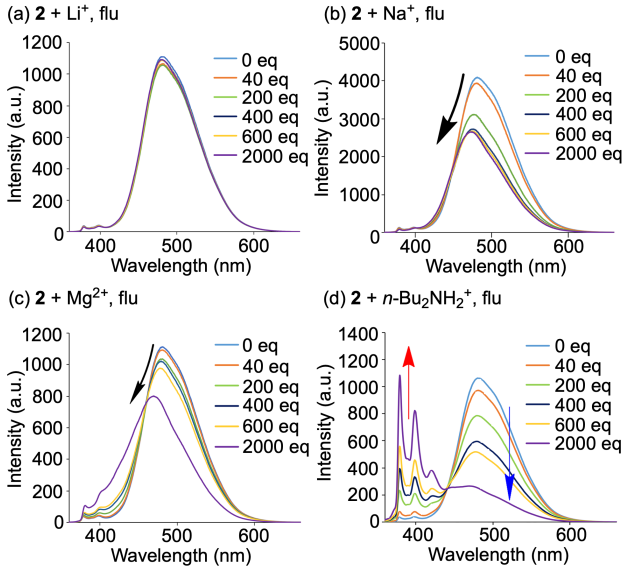

Fig. 11 Fluorescence spectra of **2** (1.0×10^{-5} M in CH_2Cl_2 : CH_3CN = 1 : 1) upon addition of (a) $LiClO_4$ (0-2000 equiv), (b) $NaClO_4$ (0-2000 equiv), (c) $Mg(ClO_4)_2$ (0-2000 equiv), and (d) n-$Bu_2NH_2^+PF_6^-$ (0-2000 equiv), λ_{ex} = (a)(c)(d) 350.5, (b) 351 nm.

Please do not adjust margins

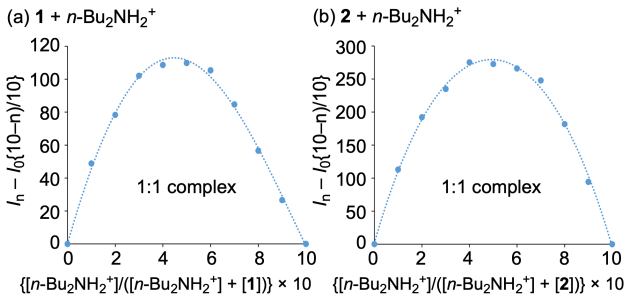

Fig. 12 Job's plot for complexation of (a) **1** and (b) **2** with *n*-$Bu_2NH_2^+PF_6^-$ obtained from change of fluorescence at 480 nm in CH_2Cl_2 : CH_3CN = 1 : 1, [**1** or **2**] + [*n*-$Bu_2NH_2^+PF_6^-$] = 1.0 × 10^{-5} M.

Cations were also added to the solution of **2**, and fluorescence spectra were evaluated under the same conditions (Fig. 11). As a result, unlike the case of **1**, it was found that the amount of change was small with Li^+, and the amount of change was large when Na^+ and Mg^{2+} were added (λ_{max} = 482 (Li^+), 473 (Na^+), and 469 (Mg^{2+}) nm). Thus, as the oligoethylene glycol chain became longer, it came to recognize metal ions with large ionic radii. Addition of Li^+ and *n*-$Bu_2NH_2^+$ to the solution of **2** did not significantly change the absorption spectrum, however, addition of Na^+ and Mg^{2+} to the solution of **2** slightly shifted the absorption band to longer wavelengths and broadened it (Fig. S5), similar to the addition of Ba^{2+} to the solution of **2** (Fig. 3b). The longer wavelength shift and broadening of the absorption of **2** by the addition of suitable-sized metal ions might be a consequence of the transannular π-π interaction[3] caused by the formation of a dumbbell-shaped complex and the distance between the pyrenes becoming closer.

To investigate the structures of species formed by mixing **1** and **2** with *n*-$Bu_2NH_2^+$ salt in solution, Job's plots were performed, and the results supported the formation of 1:1 complexes with *n*-$Bu_2NH_2^+$ for both **1** and **2** (Fig. 12). Equimolar amounts of **1** and *n*-$Bu_2NH_2^+PF_6^-$ were mixed in $CDCl_3$ and the ^1H NMR spectrum was compared with those of each alone (Fig. 13). *n*-$Bu_2NH_2^+PF_6^-$ is difficult to dissolve in $CDCl_3$, however, when mixed with pyrenophane **1**, it becomes completely soluble. In addition, splitting of the resonance of the triethylene glycol moiety and upfield shift of the *n*-butyl group were observed. A similar change was observed in the ^1H NMR spectroscopic study upon addition of *n*-$Bu_2NH_2^+$ to **2** in $CDCl_3$ (Fig. S6). These results suggested that mixing pyrenophanes **1**, **2** and *n*-$Bu_2NH_2^+$ produced pseudorotaxanes (Fig. 14).

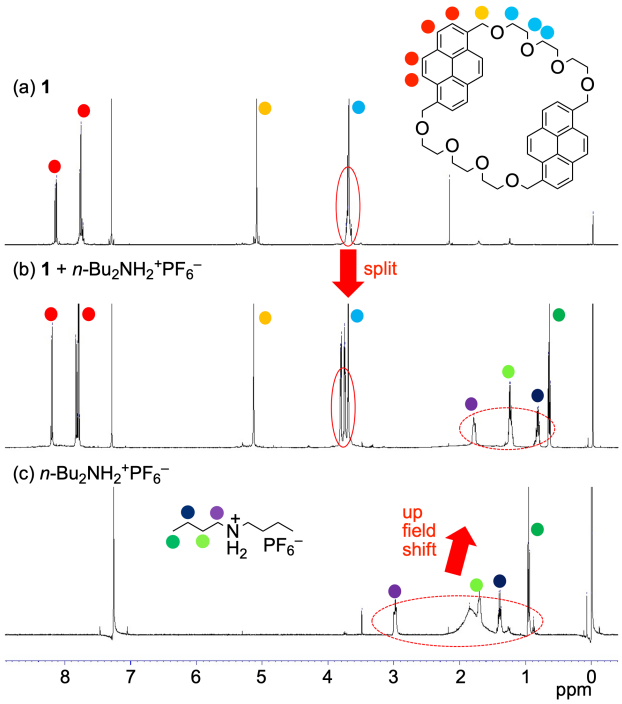

Fig. 13 500 MHz ^1H NMR spectra of (a) **1**, (b) a mixture of **1** with *n*-$Bu_2NH_2^+PF_6^-$, and (c) *n*-$Bu_2NH_2^+PF_6^-$ in $CDCl_3$.

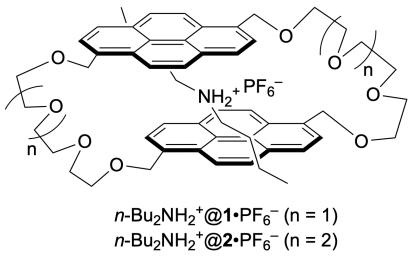

Fig. 14 Structures of pseudorotaxanes comprised of **1** and **2** with *n*-$Bu_2NH_2^+PF_6^-$.

The values of the complexation constants *K* of **1** and **2** with metal and ammonium ions obtained from the change in the fluorescence spectra are summarized in Table 1. In both **1** and **2**, the largest *K* values are obtained when Ba^{2+} was added. In addition, **1** has high affinity with Li^+ and **2** has high affinity with Na^+. In other words, as the oligoethylene glycol chain becomes longer, the ionic radius of the recognized metal ion becomes larger, which is a size matching effect. Complexation constants *K* could not be determined for the combination of **1**-Mg^{2+} and **2**-Li^+ because the amount of change in the fluorescence spectrum was too small.

This journal is © The Royal Society of Chemistry 20xx

Please do not adjust margins

Table 1 Ionic radii and complexation constants (*K*) of **1** and **2** with metal and ammonium ions.[a]

ion	ionic radius (pm)[b]	*K* (M^{-1})	
		1	**2**
Li^+	60	8.68×10^1	–[c]
Na^+	95	4.02×10^1	5.89×10^2
Mg^{2+}	65	–[c]	3.10×10^1
Ba^{2+}	135	2.26×10^3	1.95×10^5 (K_1) 2.76×10^4 (K_2)
n-$Bu_2NH_2^+$	–	9.06×10^1	1.52×10^2

[a] Complexation constants calculated by using TitrationFit 2014-0630 based on fluorescence changes. [b] Data from ref. 97. [c] Complexation constant is not available as fluorescence changes are very small.

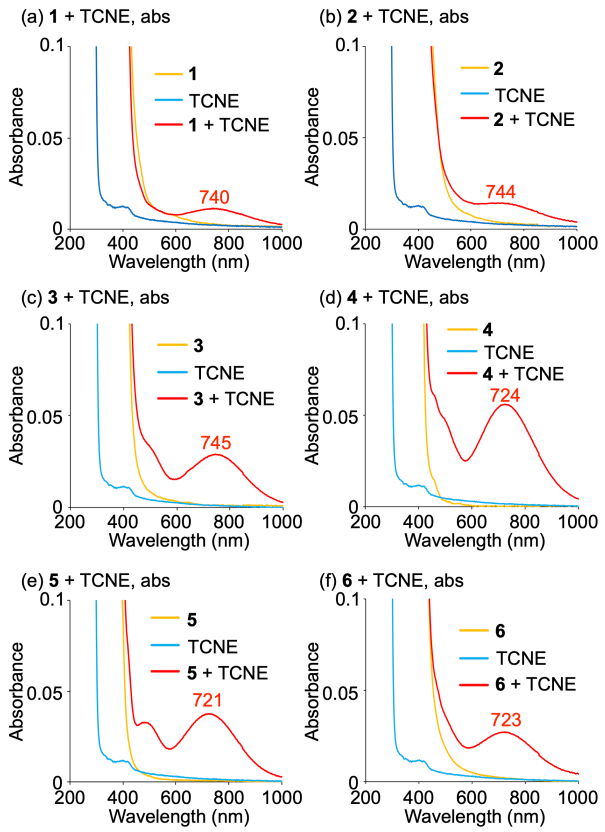

Fig. 15 UV-vis-NIR absorption spectra of **1**-**6** and TCNE in CH_2Cl_2. Yellow line: **1**-**6** (1.0×10^{-2} M), blue line: TCNE (1.0×10^{-2} M), and red line: a mixture of **1**-**6** (5.0×10^{-3} M) with TCNE (5.0×10^{-3} M).

Electron-rich pyrene is known to form a charge-transfer (CT) complex when mixed with an electron-deficient compound such as tetracyanoethylene (TCNE) in solution, exhibiting a CT-derived absorption band on the long wavelength region.[98-104] Therefore, pyrenophanes **1**, **2** were mixed with TCNE in CH_2Cl_2 solution and the absorption spectra were measured (Fig. 15). The yellow line indicates the absorption of pyrenophane alone, the blue line indicates the absorption of TCNE alone, and the red line indicates the absorption when they are mixed in an equimolar manner. In the case of **1**, a new absorption band with a peak top at 740 nm appeared, suggesting that a CT complex was formed. Similarly, pyrenophanes **2** and **3** also showed new absorption bands with peaks at respective 744 and 745 nm by mixing with TCNE. Reference compounds **4**-**6** also formed CT complexes with TCNE, however, the wavelengths were found to be about 20 nm shorter than those of pyrenophanes. Therefore, pyrenophanes **1**-**3** formed more stable CT complexes with TCNE compared to reference compounds **4**-**6**. This is a consequence of the fact that pyrenophanes **1**-**3** are more electron donating and less sterically hindered than the reference compounds **4**-**6**. From these experimental results, possible mechanism for the complexation and fluorescence is proposed in Scheme 2. First, in the absence of cations, the monomer emission of pyrenophanes **1** and **2** is very weak, showing almost exclusively intramolecular excimer emission. This is because one pyrene is excited by the excitation light and readily forms an excited dimer with the other pyrene. In the presence of metal cations, the possibility of coordination outside the pyrene ring of **1** and **2** can be excluded. This is because the resonances of the two pyrene regions in ^{1}H NMR are equivalent and the fluorescence spectra of **3** and **4** hardly change when metal ions are added.

If **1** and Ba^{2+} interact in the oligoethylene glycol chain, the symmetry of the eight hydrogens on one pyrene ring would be broken, but no such collaps of symmetry has been observed. These results indicate that **1** forms a sandwich type 1:1 complex with Ba^{2+}. When this 1:1 complex is irradiated with excitation light, Ba^{2+} spatially inhibits the formation of excited dimers, so that no intramolecular excimer fluorescence is observed, and only monomer fluorescence is observed. The possibilities of quenching due to single electron transfer (SET) from the excited singlet of pyrene in **1** to Ba^{2+} and the process of intersystem crossing (ISC) due to the external heavy atom effect[105] cannot be ruled out. However, since the decrease in fluorescence intensity is small relative to the amount of Ba^{2+} added, those paths might be negligible.

Please do not adjust margins

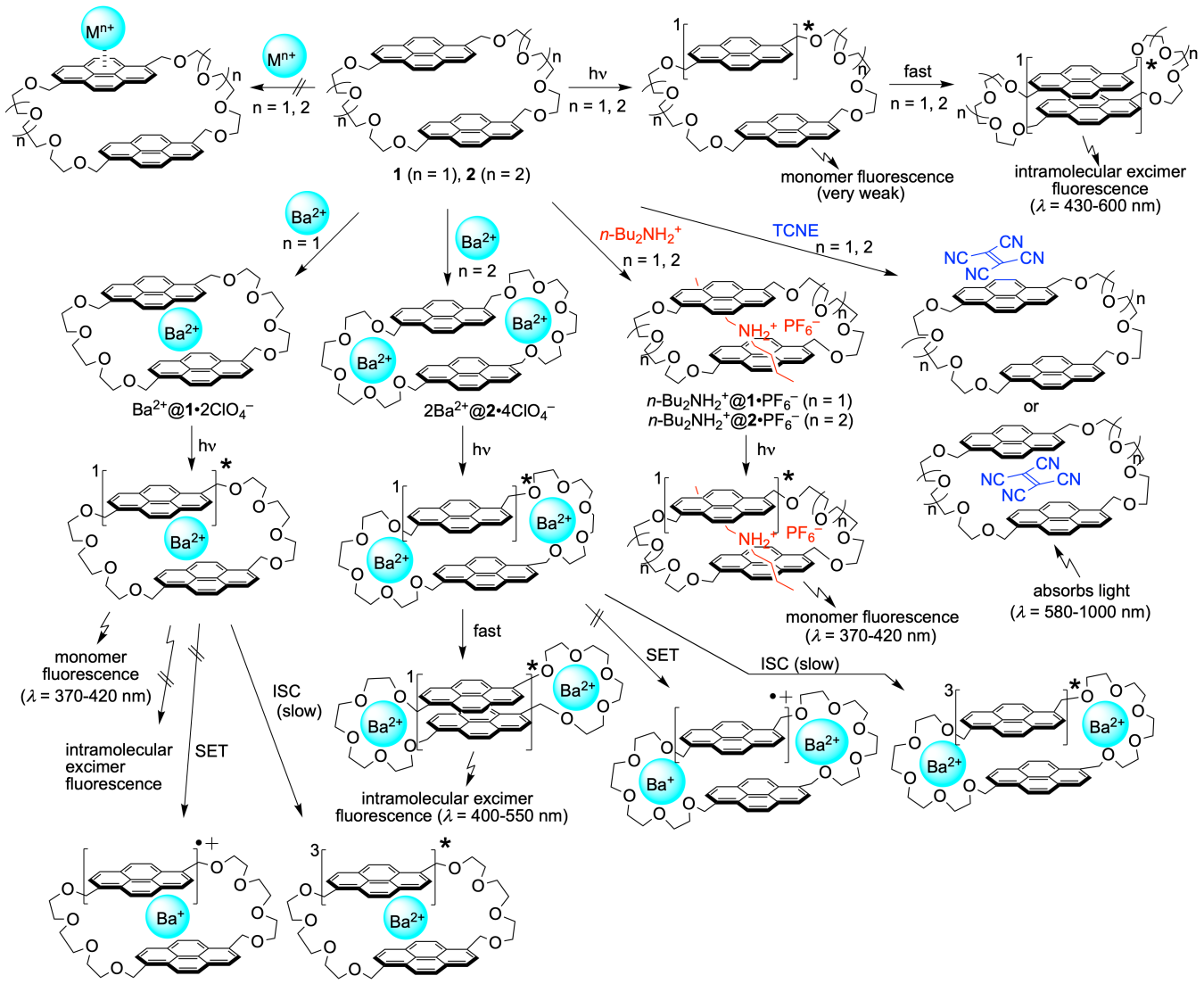

Scheme 2 Complexation and fluorescence mechanism. ^{1}[M]*, ^{3}[M]* and [M]$^{\bullet+}$ means excited singlet and triplet states and radical cation of M, respectively.

Pyrenophane **2** forms a 1:2 complex with Ba^{2+}, but unlike **1**, Ba^{2+} is in a position that does not interfere with the formation of the excited dimer of pyrene, so intramolecular excimer fluorescence is observed from the 1:2 complex. While the metal-free **2** can form an intramolecular excimer with the pyrene rings at an optimal distance, the 1:2 complex has a somewhat unreasonable intramolecular excimer with the pyrene rings in a twisted position due to the presence of Ba^{2+} ions. Therefore, the intramolecular excimer fluorescence of the 1:2 complex containing two Ba^{2+} ions appeared on the shorter wavelength region compared to that of the metal-free **2**. In other words, the addition of Ba^{2+} changed the dynamic excimer to a static excimer, resulting in a shorter wavelength shift in fluorescence.[3,16,53] In the complexation of **2** with metal ions, fluorescence quenching by SET and heavy atom effect might be negligible like **1**.

When n-$Bu_2NH_2^+$ is added to the solutions of pyrenophanes **1** and **2**, pseudorotaxane complexes are formed. Since the n-$Bu_2NH_2^+$ axis spatially prevents excimer formation, only the monomer emission is observed. When TCNE is added to the solutions of pyrenophanes, CT complexes with an absorption maximum at 740-744 nm are formed in the ground state. Since even unsubstituted pyrene interacts with TCNE to form a CT complex, it is unclear whether TCNE is present on the outside or inside of pyrenophanes.[104]

Conclusions

In summary, we synthesized (1,6)pyrenophanes **1** and **2** in which two pyrenes are linked by two oligoethylene glycol chains, and investigated the fluorescence properties when cations were added. In the absence of cations, **1** and **2** showed almost only intramolecular excimer emission. When Ba^{2+} was added to

This journal is © The Royal Society of Chemistry 20xx

Please do not adjust margins

Please do not adjust margins

the solutions of pyrenophanes, **1** showed monomer emission, while the fluorescence of **2** remained excimer emission and shifted to shorter wavelength. These fluorescence changes are attributed to the formation of sandwich-type and dumbbell-type complexes, respectively. When *n*-$Bu_2NH_2^+$ was added to the solutions of pyrenophanes, pseudorotaxane-type complexes were formed and the fluorescence changed to monomer emission. Due to their electron-donating properties and low steric hindrance, **1** and **2** formed stable CT complexes with TCNE. These (1,6)pyrenophanes linked by oligoethylene glycol chains are considered to be useful as fluorescence sensors that recognize these additives.

Experimental

Materials and equipment

$CHCl_3$ was distilled from CaH_2. CH_2Cl_2 was washed with H_2O, dried over $CaCl_2$, then distilled from CaH_2 under a nitrogen atmosphere. Toluene was distilled from CaH_2 under a nitrogen atmosphere. THF was distilled from CaH_2 and then from Na and $Ph_2C{=}O$ under a nitrogen atmosphere. DMF was distilled without using a drying agent. Anhydrous grade of CH_2Cl_2, toluene, and THF were also purchased and used without further purification. Spectral grade solvents were used for spectroscopic studies. Most liquid substances were used after purification by distillation. Most solid substances were used as purchased. Melting points were determined on a Gallenkamp MFB-595 melting point apparatus. ^{1}H and ^{13}C NMR spectra were recorded using a JEOL JMN LA-400 (400 MHz and 100 MHz, respectively) or a JEOL ECA-500 (500 MHz and 125 MHz, respectively) spectrometer with Me_4Si as an internal standard. IR spectra were determined using a Shimadzu FTIR-8300 spectrometer. Low- and high-resolution mass spectra were taken on a JEOL JMS-700 instrument. UV-vis absorption spectra were recorded using a Hitachi U-2900 or a JASCO V-570 spectrophotometer. Fluorescence spectra were recorded using a JASCO FP-8500 spectrophotometer (Ex slit: 2.5 nm, Em slit: 2.5 nm, scanning speed: 500 nm/min, response: 50 msec). HPLC separations were performed on a recycling preparative HPLC instrument (Japan Analytical Industry Co. Ltd., LC-908 equipped with a JAIGEL-H (GPC) column). Column chromatography was conducted by using Kanto Chemical Co. Ltd., silica gel 60 N (spherical, neutral, 0.04-0.05 mm). Thin-layer chromatography was performed with Merck Kiesel gel 60 F_{254} plates, and bands were detected by using UV light and a phosphomolybdic acid ethanol solution with heating.

Pyrenophane 1

To a stirred CCl_4 (150 mL) solution of pyrene (**7**, 6.058 g, 30 mmol) was added dropwise a CCl_4 (40 mL) solution of Br_2 (3.08 mL, 60 mmol) over a 2 h period at room temperature, and the solution was stirred for 12 h at room temperature.[106] To the solution was added 1 N NaOH aqueous solution (50 mL) to give white solid. The solid was collected by filtration, washed with EtOH, and dried overnight at room temperature. The solid was dissolved in hot toluene and filtered to remove tribromo- and tetrabromo-pyrenes. The filtrate was concentrated in vacuo to give a residue. Recrystallization from toluene gave pale yellow solid of a mixure of 1,6-dibromopyrene (**8**) : 1,8-dibromopyrene = 4 : 1. Recrystallization from toluene again gave pure 1,6-dibromopyrene (**8**, 2.305 g, 22% yield). Pale yellow solid; ^{1}H NMR (400 MHz, $CDCl_3$) δ 8.07 (d, *J* = 8.3 Hz, 2H), 8.14 (d, *J* = 9.3 Hz, 2H), 8.28 (d, *J* = 8.3 Hz, 2H), 8.48 (d, *J* = 9.3 Hz, 2H) ppm. Lit.[107]

To a stirred THF (60 mL) solution of 1,6-dibromopyrene (**8**, 2.16 g, 6.0 mmol) was added dropwise *t*-BuLi (1.69 M in *n*-hexane, 16.4 mL, 27 mmol) at –78 °C under an argon atmosphere, and the solution was stirred at –78 °C for 1 h. To the solution was added dropwise DMF (4.6 mL, 60 mmol), and the solution was stirred at –78 °C for 1 h, and then at room temperature for 1 h.[108] To the solution was added H_2O (50 mL). The formed solid was collected by filtration, washed with H_2O (30 mL), MeOH (30 mL), and hot toluene (30 mL) to give 1,6-diformylpyrene (**9**, 1.311 g, 85% yield). Yellow solid; ^{1}H NMR (500 MHz, $CDCl_3$) δ 8.36 (d, *J* = 9.2 Hz, 2H), 8.43 (d, *J* = 8.0 Hz, 2H), 8.55 (d, *J* = 7.4 Hz, 2H), 9.59 (d, *J* = 9.2 Hz, 2H), 10.82 (s, 2H) ppm. Lit.[103]

To a stirred THF (110 mL) solution of 1,6-diformylpyrene (**9**, 1.449 g, 5.6 mmol) were added $NaBH_4$ (0.849 g, 22.4 mmol) and EtOH (25 mL), and the mixture was stirred at room temperature for 18 h.[109] To the solution was added 1 N HCl aqueous solution (40 mL) to give white solid. The solid was collected by filtration, washed with Et_2O (40 mL) and $CHCl_3$ (40 mL) to give 1,6-bis(hydroxymethyl)pyrene (**10**, 1.371 g, 93% yield). White solid; ^{1}H NMR (500 MHz, $CDCl_3$) δ 5.44 (s, 4H), 8.09 (d, *J* = 8.0 Hz, 2H), 8.16 (d, *J* = 9.2 Hz, 2H), 8.21 (d, *J* = 7.5 Hz, 2H), 8.40 (d, *J* = 9.2 Hz, 2H) ppm. Lit.[110]

To a stirred CH_3CN (130 mL) solution of 1,6-bis(hydroxymethyl)pyrene (**10**, 0.658 g, 2.5 mmol) were added NaI (2.25 g, 15.0 mmol) and Me_3SiCl (1.90 mL, 15.0 mmol), and the solution was stirred at room temperature for 2 h.[111] To the solution was added H_2O (100 mL). The formed yellow solid was washed with H_2O (50 mL) to give 1,6-bis(iodomethyl)pyene (**11**, 1.111 g, 92% yield). Yellow solid; ^{1}H NMR (500 MHz, $CDCl_3$) δ 5.21 (s, 4H), 8.05 (d, *J* = 8.0 Hz, 2H), 8.16 (d, *J* = 8.0 Hz, 2H), 8.22 (d, *J* = 9.2 Hz, 2H), 8.34 (d, *J* = 9.2 Hz, 2H) ppm. Lit.[112]

A mixture of triethylene glycol (0.18 mL, 1.35 mmol), NaH (60% in mineral oil, 0.48 g, 20.0 mmol), and THF (60 mL) was stirred at reflux for 1 h under an argon atmosphere. To the solution was added dropwise a mixture of 1,6-bis(iodomethyl)pyene (**11**, 0.460 g, 0.95 mmol) and THF (40 mL) over a 5 min period, and the solution was stirred at reflux for 3 days.[113] To the solution were added H_2O (100 mL) and 1 N HCl aqueous solution (20 mL). The product was extracted with $CHCl_3$ (100 mL × 3). The combined organic layers were washed with 1 N HCl (100 mL), dried over Na_2SO_4, filtered, and concentrated in vacuo, giving a residue that was subjected to silica gel column chromatography (eluent; $CHCl_3$: EtOH = 30 : 1, R_f = 0.4) followed by recycling preparative HPLC (GPC, eluent; $CHCl_3$) to give 2,5,8,11,24,27,30,33-octaoxa[12.12](1,6)pyrenophane (**1**, 0.018 g, 3 % yield). Pale yellow solid; mp 185-187 °C; ^{1}H NMR (500MHz, $CDCl_3$) δ 3.69 (d, *J* = 4.0 Hz, 24H), 4.96 (s, 8H), 7.70-

Please do not adjust margins

7.75 (m, 12H), 8.10 (d, *J* = 9.2 Hz, 4H) ppm; ^{13}C NMR (125 MHz, $CDCl_3$) δ 69.67, 70.89, 70.95, 71.74, 123.14, 124.37, 124.59, 126.76, 127.32, 129.13, 130.53, 131.28 ppm; IR (KBr) 845, 1096, 1299, 1346, 2862 cm^{-1}; MS (FAB+) *m/z* (relative intensity, %) = 136 (65), 154 (100), 307 (29), 753 (M$^+$, 3); HRMS (FAB+) calcd for $C_{48}H_{49}O_8$: 753.3427, found: 753.3421.

Pyrenophanes 2 and 3

A mixture of tetraethylene glycol (0.19 mL, 1.1 mmol), NaH (60% in mineral oil, 0.48 g, 20.0 mmol), and THF (60 mL) was stirred at reflux for 1 h under an argon atmosphere. To the solution was added dropwise a mixture of 1,6-bis(iodomethyl)pyene (**11**, 0.482 g, 1.1 mmol, see preparation of **1**) and THF (50 mL) over a 5 min period, and the solution was stirred at reflux for 3 days.[113] To the solution were added H_2O (50 mL) and 1 N HCl aqueous solution (20 mL). The product was extracted with $CHCl_3$ (100 mL × 3). The combined organic layers were washed with 1 N HCl (100 mL), dried over Na_2SO_4, filtered, and concentrated in vacuo, giving a residue that was subjected to silica gel column chromatography (eluent; $CHCl_3$: EtOH = 30 : 1, R_f = 0.4-0.5) followed by recycling preparative HPLC (GPC, eluent; $CHCl_3$) to give 2,5,8,11,14,27,30,33,36,39-decaoxa[15.15](1,6)pyrenophane (**2**, 0.022 g, 3% yield) and 2,5,8,11,14-pentaoxa[15](1,6)pyrenophane (**3**, 0.015 g, 4% yield). Data for **2**; pale yellow solid; mp 149-152 °C, ^{1}H NMR (500MHz, $CDCl_3$) δ 3.55-3.63 (m, 32H), 5.05 (s, 8H), 7.79 (d, *J* = 8.0 Hz, 4H), 7.86 (d, *J* = 9.2 Hz, 4H), 7.91 (d, *J* = 8.0 Hz, 4H), 8.13 (d, *J* = 9.2 Hz, 4H) ppm; ^{13}C NMR (125 MHz, $CDCl_3$) δ69.51, 70.67, 70.71, 71.75, 123.30, 124.49, 124.71, 126.93, 127.49, 129.26, 130.69, 131.41 ppm; IR (KBr) 845, 1096, 1246, 1357, 2866 cm^{-1}; MS (FAB+) *m/z* (relative intensity, %) = 77 (11), 107 (16), 154 (100), 307 (26), 841 (M$^+$, 1); HRMS (FAB+) calcd for $C_{52}H_{57}O_{10}$: 841.3952, found: 841.3939. Data for **3**; pale yellow solid; mp 123-126 °C; ^{1}H NMR (500MHz, $CDCl_3$) δ 1.63-1.68 (m, 2H), 2.09-2.13 (m, 2H), 2.39-2.44 (m, 2H), 2.49-2.52 (m, 2H), 3.12-3.15 (m, 2H), 3.27-3.29 (m, 2H), 3.47-3.51 (m, 2H), 3.68-3.72 (m, 2H), 4.73 (d, *J* = 13.2 Hz, 2H), 5.85 (d, *J* = 13.2 Hz, 2H), 7.96 (d, *J* = 7.4 Hz, 2H), 8.16 (d, *J* = 9.2 Hz, 2H), 8.17 (d, *J* = 7.5 Hz, 2H), 8.57 (d, *J* = 9.2 Hz, 2H) ppm; ^{13}C NMR (125 MHz, $CDCl_3$) δ 68.19, 68.33, 69.06, 70.31, 72.18, 124.32, 124.75, 125.19, 127.40, 128.50, 130.28, 131.22, 132.23 ppm; IR (KBr) 848, 1087, 1249, 1361, 2858 cm^{-1}; MS (FAB+) *m/z* (relative intensity, %) = 73 (20), 85 (17), 119 (26), 154 (30), 189 (5), 215 (39), 228 (76), 243 (35), 288 (7), 324 (8), 421 (M$^+$, 1); HRMS (FAB+) calcd for $C_{26}H_{29}O_5$: 421.2015, found: 421.2010.

1,6-Bis(methoxymethyl)pyrene (4)

A mixture of 1,6-bis(hydroxymethyl)pyrene (**10**, 0.079 g, 0.3 mmol, see preparation of **1**), NaH (60% in mineral oil, 0.072 g, 3.0 mmol), and THF (20 mL) was stirred at reflux for 1 h under a nitrogen atmosphere. To the solution was added dropwise MeI (0.112 mL, 1.8 mmol), and the solution was stirred at reflux for 2 days.[77] To the solution was added H_2O (50 mL), and the solution was concentrated by a rotary evaporator to remove THF. The product was extracted with CH_2Cl_2 (30 mL × 3) from the aqueous solution. The combined organic layers were washed with brine (30 mL), dried over Na_2SO_4, filtered, and concentrated in vacuo, giving a residue that was subjected to silica gel column chromatography (eluent; $CHCl_3$: EtOH = 30 : 1, R_f = 0.7) followed by recycling preparative HPLC (GPC, eluent; $CHCl_3$) to give 1,6-bis(methoxymethyl)pyrene (**4**, 0.044 g, 51% yield). Yellow solid; ^{1}H NMR (500 MHz, $CDCl_3$) δ 3.52 (s, 6H), 5.18 (s, 4H), 8.03 (d, *J* = 8.0 Hz, 2H), 8.13 (d, *J* = 9.2 Hz, 2H), 8.17 (d, *J* = 8.1 Hz, 2H), 8.35 (d, *J* = 9.2 Hz, 2H) ppm. Lit.[114,115]

Compound 5

To a stirred CH_2Cl_2 (150 mL) solution of pyrene (**7**, 3.11 g, 15.0 mmol) were added dropwise CH_3OCHCl_2 (1.80 mL, 19.5 mmol) and $TiCl_4$ (27 mL, 27.0 mmol) at 0 °C under an argon atmosphere, and the solution was stirred at 0 °C for 1 h, then at room temperature for 1.5 h.[116] To the solution was added cool water. The organic layer was separated. The aqueous layer was washed with CH_2Cl_2 (100 mL × 3). The combined organic layers were washed with brine (100 mL), dried over Na_2SO_4, filtered, and concentrated in vacuo, giving a residue that was subjected to silica gel column chromatography (eluent; CH_2Cl_2) to give 1-formylpyrene (**14**, 3.410 g, 99% yield). Yellow green solid; ^{1}H NMR (500 MHz, $CDCl_3$) δ 8.06-8.11 (m, 2H), 8.21-8.32 (m, 5H), 8.43 (d, *J* = 8.0 Hz, 1H), 9.41 (d, *J* = 9.2 Hz, 1H), 10.77 (s, 1H) ppm. Lit.[116]

To a stirred THF (120 mL) solution of 1-formylpyrene (**14**, 0.919 g, 4.0 mmol) were added $NaBH_4$ (0.303 g, 8.0 mmol) and EtOH (20 mL) at 0 °C, and the mixture was stirred at room temperature for 16 h.[109] To the solution was added 1 N HCl aqueous solution (50 mL). The organic layer was separated. The aqueous layer was washed with Et_2O (100 mL × 3). The combined organic layers were washed with brine (100 mL), dried over Na_2SO_4, filtered, and concentrated in vacuo to give 1-(hydroxymethyl)pyrene (**15**, 0.965 g, 100% yield, including impurity). Yellow solid, ^{1}H NMR (400 MHz, $CDCl_3$) δ 1.83 (brs, 1H), 5.39 (s, 2H), 7.99-8.08 (m, 4H), 8.12-8.22 (m, 4H), 8.36 (d, *J* = 9.3 Hz, 1H) ppm. Lit.[117]

To a stirred $CHCl_3$ (40 mL) solution of 1-(hydroxymethyl)pyrene (**15**, 0.872 g, 4.1 mmol, including impurity) was added dropwise PBr_3 (0.39 mL, 4.1 mmol) at 0 °C under an argon atmosphere, and the solution was stirred at room temperature for 20 h.[110] To the solution was added saturated NH_4Cl aqueous solution (40 mL). The organic layer was separated. The aqueous layer was washed with $CHCl_3$ (50 mL × 3). The combined organic layers were washed with brine (50 mL), dried over Na_2SO_4, filtered, and concentrated in vacuo to give 1-(bromomethyl)pyrene (**16**, 1.207 g, 99% yield). Yellow solid; ^{1}H NMR (500 MHz, $CDCl_3$) δ 5.27 (s, 2H), 8.02-8.06 (m, 3H), 8.08-8.14 (m, 2H), 8.21-8.27 (m, 3H), 8.39 (d, *J* = 9.2 Hz, 1H) ppm. Lit.[116]

A mixture of triethylene glycol (0.10 mL, 0.5 mmol), NaH (60% in mineral oil, 0.48 g, 20.0 mmol), and THF (50 mL) was stirred at reflux for 1 h under an argon atmosphere. To the solution was added dropwise THF (30 mL) solution of 1-(bromomethyl)pyrene (**16**, 0.295 g, 1.0 mmol) over a 30 min period, and the solution was stirred at reflux for 3 days.[113] To

 This journal is © The Royal Society of Chemistry 20xx

Please do not adjust margins

the solution was added H_2O. The organic layer was separated. The aqueous layer was washed with $CHCl_3$ (100 mL × 3). The combined organic layers were washed with brine (100 mL), dried over Na_2SO_4, filtered, and concentrated in vacuo, giving a residue that was subjected to silica gel column chromatography (eluent; $CHCl_3$: EtOH = 30 : 1, R_f = 0.3) followed by recycling preparative HPLC (GPC, eluent; $CHCl_3$) to give triethylene glycol bis(pyren-1-ylmethyl) ether (**5**, 0.076 g, 13% yield). Yellow soild; ^{1}H NMR (500 MHz, $CDCl_3$) δ3.71-3.68 (m, 12H), 5.23 (s, 4H), 8.14 (d, *J* = 8.0 Hz, 2H), 8.15 (d, *J* = 8.0 Hz, 2H), 8.35 (d, *J* = 9.2 Hz, 2H) ppm. Lit.[77]

Compound 6

A mixture of tetraethylene glycol (0.09 mL, 0.5 mmol), NaH (60% in mineral oil, 0.48 g, 20.0 mmol), and THF (50 mL) was stirred at reflux for 1 h under an argon atmosphere. To the solution was added dropwise THF (30 mL) solution of 1-(bromomethyl)pyrene (**16**, 0.295 g, 1.0 mmol, see preparation of **5**) over a 30 min period, and the solution was stirred at reflux for 3 days.[113] To the solution was added H_2O. The organic layer was separated. The aqueous layer was washed with $CHCl_3$ (100 mL × 3). The combined organic layers were washed with brine (100 mL), dried over Na_2SO_4, filtered, and concentrated in vacuo, giving a residue that was subjected to silica gel column chromatography (eluent; $CHCl_3$: EtOH = 30 : 1, R_f = 0.3) followed by recycling preparative HPLC (GPC, eluent; $CHCl_3$) to give tetraethylene glycol bis(pyren-1-ylmethyl) ether (**6**, 0.081 g, 13% yield). Yellow oil; ^{1}H NMR (500 MHz, $CDCl_3$) δ3.61-3.71 (m, 16H), 5.21 (s, 4H), 7.94-8.02 (m, 8H), 8.08 (d, *J* = 8.6 Hz, 4H), 8.14 (d, *J* = 8.0 Hz, 2H), 8.14 (d, *J* = 7.5 Hz, 2H), 8.34 (d, *J* = 9.2 Hz, 2H) ppm. Lit.[77]

Compounds 12 and 13

A mixture of diethylene glycol (0.05 mL, 0.55 mmol), NaH (60% in mineral oil, 0.06 g, 2.5 mmol), and THF (40 mL) was stirred at reflux for 1 h under an argon atmosphere. To the solution was added dropwise THF (30 mL) solution of 1,6-bis(iodomethyl)pyrene (**11**, 0.241 g, 0.5 mmol, see preparation of **1**), and the solution was stirred at reflux for 3 days.[113] To the solution was added H_2O (100 mL) and 1 N HCl aqueous solution (20 mL). The organic layer was separated. The aqueous layer was washed with $CHCl_3$ (100 mL × 3). The combined organic layers were washed with 1 N HCl aqueous solution (100 mL), dried over Na_2SO_4, filtered, and concentrated in vacuo. The residue was filtered through silica gel and subjected to recycling preparative HPLC (GPC, eluent; $CHCl_3$) to give 1,6-bis[2-(2-hydroxyethoxy)ethoxymethyl]pyrene (**12**, 0.030 g, 13% yield) and triethylene glycol bis{6-[2-(2-hydroxyethoxy)ethoxymethyl]pyren-1-ylmethyl} ether (**13**, 0.018 g, 5% yield). Data for **12**; orange solid; mp 67-73 °C; ^{1}H NMR (500 MHz, $CDCl_3$) δ3.61 (t, *J* = 4.6 Hz, 4H), 3.73 (dd, *J* = 4.3, 3.4 Hz, 8H), 3.76 (t, *J* = 2.6 Hz, 4H), 5.30 (s, 4H), 8.04 (d, *J* = 7.4 Hz, 2H), 8.13 (d, *J* = 9.2 Hz, 2H), 8.17 (d, *J* = 8.0 Hz, 2H), 8.39 (d, *J* = 9.0 Hz, 2H) ppm; ^{13}C NMR (125 MHz, $CDCl_3$) δ61.84, 69.47, 70.50, 71.95, 72.38, 123.46, 124.79, 125.00, 127.24, 127.75, 129.55, 131.02, 131.30 ppm; IR (KBr) 883, 1072, 1354, 1654, 2901, 3483 cm^{-1}; MS (FAB+) *m/z* (relative intensity, %) = 57 (33), 85 (26), 119 (41), 154 (39), 215 (18), 228 (29), 333 (100), 438 (M^+, 1); HRMS (FAB+) calcd for $C_{48}H_{50}O_9$: 438.2042, found: 438.2052. Data for **13**; orange solid; ^{1}H NMR (500 MHz, $CDCl_3$) δ 3.61 (t, *J* = 4.6 Hz, 4H), 3.68-3.76 (m, 16H), 3.76-3.79 (m, 4H), 3.78 (d, *J* = 5.5 Hz, 4H), 5.23 (s, 4H), 5.24 (s, 4H), 7.92-8.06 (m, 12H), 8.29 (d, *J* = 9.2 Hz, 4H) ppm; ^{13}C NMR (125 MHz, $CDCl_3$) δ 61.82, 69.44, 69.60, 70.48, 70.91, 71.88, 71.94, 72.43, 123.20, 123.50, 124.58, 124.68, 124.84, 127.01, 127.13, 127.51, 127.65, 129.39, 129.41, 130.80, 130.88, 131.04, 131.59 ppm; IR (KBr) 883, 1072, 1354, 1654, 2901, 3483 cm^{-1}; MS (FAB+) *m/z* (relative intensity, %) = 73 (17), 102 (46), 154 (81), 228 (65), 333 (100), 665 (21), 770 (M^+, 12); HRMS (FAB+) calcd for $C_{48}H_{50}O_9$: 770.3455, found: 770.3456.

Conflicts of interest

There are no conflicts to declare.

Acknowledgements

This study was financially supported by a Grant-in-Aid for Scientific Research (C) (23550047, 26410040, 17K05777, 20K05474) from the Ministry of Education, Culture, Sports, Science and Technology (MEXT) of Japan. This study was also supported by the Murata Science Foundation, Izumi Science and Technology Foundation, Shibuya Science Culture and Sports Foundation, Iketani Science and Technology Foundation, Fukuoka Naohiko Memorial Foundation, The Mitani Foundation for Research and Development, A-STEP (Adaptable and Seamless Technology Transfer Program through target-driven R&D, JST, Japan), and Kanazawa University SAKIGAKE Project. We are also indebted to Prof. Shigehisa Akine at Kanazawa University for providing TitrationFit 2014-0630 program, and Professor Tsuyoshi Asakawa and Associate Professor Akio Ohta at Kanazawa University for permission to use a UV-vis absorption spectrophotometer (Hitachi U-2900).

Notes and references

1 J. B. Birks, *Acta Phys. Pol.*, 1968, **34**, 603–617.
2 Th. Förster, *Angew. Chem. Int. Ed.*, 1969, **8**, 333–343.
3 F. M. Winnik, *Chem. Rev.*, 1993, **93**, 587–614.
4 S. Karuppannan and J.-C. Chambron, *Chem. Asian J.*, 2011, **6**, 964–984.
5 M. E. Østergaard and P. J. Hrdlicka, *Chem. Soc. Rev.*, 2011, **40**, 5771–5788.
6 T. M. Figueira-Duarte and K. Müllen, *Chem. Rev.*, 2011, **111**, 7260–7314.
7 E. Manandhar and K. J. Wallace, *Inorg. Chim. Acta*, 2012, **381**, 15–43.
8 J. Duhamel, *Langmuir*, 2012, **28**, 6527–6538.
9 J. J. Bryant and U. H. F. Bunz, *Chem. Asian J.*, 2013, **8**, 1354–1367.
10 J. M. Casas-Solvas, J. D. Howgego and A. P. Davis, *Org. Biomol. Chem.*, 2014, **12**, 212–232.
11 Y. Gong, X. Zhan, Q. Li and Z. Li, *Sci. Chin. Chem.*, 2016, **59**, 1623–1631.

Please do not adjust margins

12 X. Feng, J.-Y. Hu, C. Redshaw and T. Yamato, *Chem. Eur. J.*, 2016, **22**, 11898–11916.
13 D. Zych, *Molecules*, 2019, **24**, 2551.
14 Y. Ohishi and M. Inouye, *Tetrahedron Lett.*, 2019, **60**, 151232.
15 F. Dumur, *Eur. Polym. J.*, 2020, **126**, 109564.
16 Z. Kowser, U. Rayhan, T. Akther, C. Redshaw and T. Yamato, *Mater. Chem. Front.*, 2021, **5**, 2173–2200.
17 F. P. Kinik, A. Ortega-Guerrero, D. Ongari, C. P. Ireland and B. Smit, *Chem. Soc. Rev.*, 2021, **50**, 3143–3177.
18 K. Ayyavoo and P. Velusamy, *New J. Chem.*, 2021, **45**, 10997–11017.
19 M. Shellaiah and K.-W. Sun, *Biosensors*, 2022, **12**, 550.
20 P. G. Ghasemabadi, T. Yao and G. J. Bodwell, *Chem. Soc. Rev.*, 2015, **44**, 6494–6518.
21 T. Kawashima, T. Otsubo, Y. Sakata and S. Misumi, *Tetrahedron Lett.*, 1978, **19**, 5115–5118.
22 H. A. Staab and R. G. H. Kirrstetter, *Liebigs Ann. Chem.*, 1979, 886–898.
23 A. Terahara, H. Ohya-Nishiguchi, N. Hirota, Y. Sakata, S. Misumi and K. Ishizu, *Bull. Chem. Soc. Jpn.*, 1982, **55**, 3896–3898.
24 M. Inouye, K. Fujimoto, M. Furusyo and H. Nakazumi, *J. Am. Chem. Soc.*, 1999, **121**, 1452–1458.
25 H. Abe, Y. Mawatari, H. Teraoka, K. Fujimoto and M. Inouye, *J. Org. Chem.*, 2004, **69**, 495–504.
26 H. Hayashi, N. Matsumura and K. Mizuno, *J. Chem. Res.*, 2004, 599–601.
27 K. Imai, S. Hatano, A. Kimoto, J. Abe, Y. Tamai and N. Nemoto, *Tetrahedron*, 2010, **66**, 8012–8017.
28 Y. Sagara and N. Tamaoki, *RSC Adv.*, 2017, **7**, 47056–47062.
29 R. Mannancherry, M. Devereux, D. Häussinger and M. Mayor, *J. Org. Chem.*, 2019, **84**, 5271–5276.
30 Y. Sagara, H. Traeger, J. Li, Y. Okado, S. Schrettl, N. Tamaoki and C. Weder, *J. Am. Chem. Soc.*, 2021, **143**, 5519–5525.
31 K. Takaishi, S. Murakami, F. Yoshinami and T. Ema, *Angew. Chem. Int. Ed.*, 2022, **61**, e202204609.
32 T. Umemoto, S. Satani, Y. Sakata and S. Misumi, *Tetrahedron Lett.*, 1975, **16**, 3159–3162.
33 R. H. Mitchell, R. J. Carruthers and J. C. M. Zwinkels, *Tetrahedron Lett.*, 1976, **17**, 2585–2588.
34 H. Irngartinger, R. G. H. Kirrstetter, C. Krieger, H. Rodewald and H. A. Staab, *Tetrahedron Lett.*, 1977, **18**, 1425–1428.
35 K. Ishizu, Y. Sugimoto, T. Umemoto, Y. Sakata and S. Misumi, *Bull. Chem. Soc. Jpn.*, 1977, **50**, 2801–2802.
36 Y. Kai, F. Hama, N. Yasuoka and N. Kasai, *Acta Cryst.*, 1978, **B34**, 1263–1270.
37 S. Ishikawa, J. Nakamura, S. Iwata, M. Sumitani, S. Nagakura, Y. Sakata and S. Misumi, *Bull. Chem. Soc. Jpn.*, 1979, **52**, 1346–1350.
38 H. A. Staab, N. Riegler, F. Diederich, C. Krieger and D. Schweitzer, *Chem. Ber.*, 1984, **117**, 246–259.
39 P. Reynders, W. Kühnle and K. A. Zachariasse, *J. Am. Chem. Soc.*, 1990, **112**, 3929–3939.
40 T. Umemoto, T. Kawashima, Y. Sakata and S. Misumi, *Chem. Lett.*, 1975, **4**, 837–840.
41 T. Hayashi, N. Mataga, Y. Sakata and S. Misumi, *Chem. Phys. Lett.*, 1976, **41**, 325–328.
42 T. Hayashi, N. Mataga, T. Umemoto, Y. Sakata and S. Misumi, *J. Phys. Chem.*, 1977, **81**, 424–429.
43 T. Yamato, A. Miyazawa and M. Tashiro, *J. Chem. Soc. Perkin Trans. 1*, 1993, 3127–3137.
44 H. Maeda, M. Hironishi, R. Ishibashi, K. Mizuno and M. Segi, *Photochem. Photobiol. Sci.*, 2017, **16**, 228–237.
45 H. Maeda, K. Nakamura, T. Furuyama and M. Segi, *Photochem. Photobiol. Sci.*, 2019, **18**, 2397–2410.
46 H. Maeda, M. Geshi, K. Hirose, T. Furuyama and M. Segi, *Tetrahedron*, 2019, **75**, 130512.
47 K. S. Unikela, B. L. Merner, P. G. Ghasemabadi, C. C. Warford, C. S. Qiu, L. N. Dawe, Y. Zhao and G. J. Bodwell, *Eur. J. Org. Chem.*, 2019, 4546–4560.
48 P. G. Ghasemabadi, Y. Zhao and G. J. Bodwell, *Eur. J. Org. Chem.*, 2021, 3559–3568.
49 K. S. Unikela, Z. A. Tabasi, L. N. Dawe, Y. Zhao and G. J. Bodwell, *J. Org. Chem.*, 2021, **86**, 4405–4412.
50 H.-F. Ji, R. Dabestani, G. M. Brown and R. L. Hettich, *Photochem. Photobiol.*, 1999, **69**, 513–516.
51 H. Takemura, H. Nakamichi and K. Sako, *Tetrahedron Lett.*, 2005, **46**, 2063–2066.
52 S. Nath and U. Maitra, *Org. Lett.*, 2006, **8**, 3239–3242.
53 E. J. Jun, H. N. Won, J. S. Kim, K.-H. Lee and J. Yoon, *Tetrahedron Lett.*, 2006, **47**, 4577–4580.
54 Z. Wang, S. H. Chang and T. J. Kang, *Spectrochimica Acta A*, 2008, **70**, 313–317.
55 Ü. Ocak, M. Ocak, A. Basoglu, S. Parlayan, H. Alp and H. Kantekin, *J. Incl. Phenom. Macrocycl. Chem.*, 2010, **67**, 19–27.
56 Ü. Ocak, M. Ocak, S. Parlayan, A. Basoglu, Y. Caglar and Z. Bahadir, *J. Lumin.*, 2011, **131**, 808–814.
57 R. S. Kathayat and N. S. Finney, *J. Am. Chem. Soc.*, 2013, **135**, 12612–12614.
58 Z. Li, W. Li, F. Liu and X. Wang, *J. Phys. Org. Chem.*, 2017, e3792.
59 T. Jao, G. S. Beddard, P. Tundo, J. H. Fendler, *J. Phys. Chem.*, 1981, **85**, 1963–1966.
60 S. H. Kim, K. C. Song, S. Ahn, Y. S. Kang and S.-K. Chang, *Tetrahedron Lett.*, 2006, **47**, 497–500.
61 M. G. Choi, H. J. Kim and S.-K. Chang, *Bull. Korean Chem. Soc.*, 2008, **29**, 567–570.
62 H.-F. Wang and S.-P. Wu, *Tetrahedron*, 2013, **69**, 1965–1969.
63 V. Merz, J. Merz, M. Kirchner, J. Lenhart, T. B. Marder and Krueger, *Chem. Eur. J.*, 2021, **27**, 8118–8126.
64 K. Kubo and T. Sakurai, *Chem. Lett.*, 1996, **25**, 959–960.
65 Y. Suzuki, T. Morozumi, H. Nakamura, M. Shimomura, T. Hayashita and R. A. Bartsh, *J. Phys. Chem. B*, 1998, **102**, 7910–7917.
66 S. Nishizawa, M. Watanabe, T. Uchida and N. Teramae, *J. Chem. Soc. Perkin Trans. 2*, 1999, 141–143.
67 I. Suzuki, M. Ito, T. Osa and J. Anzai, *Chem. Pharm. Bull.*, 1999, **47**, 151–155.
68 A. Yamauchi, T. Hayashita, A. Kato, S. Nishizawa, M. Watanabe and N. Teramae, *Anal. Chem.*, 2000, **72**, 5841–5846.
69 J.-Y. Li, L.-P. Zhang, L.-Z. Wu, B.-J. Wang and C.-H. Tung, *Chin. J. Chem.*, 2001, **19**, 960–965.
70 A. Yamauchi, T. Hayashita, A. Kato and N. Teramae, *Bull. Chem. Soc. Jpn.*, 2002, **75**, 1527–1532.
71 Y. Nakahara, Y. Matsumi, W. Zhang, T. Kida, Y. Nakatsuji and I. Ikeda, *Org. Lett.*, 2002, **4**, 2641–2644.
72 H. Itagaki, W. Masuda, Y. Hirayanagi and K. Sugimoto, *J. Phys. Chem. B*, 2002, **106**, 3316–3322.
73 D. Y. Sasaki, T. A. Waggoner, J. A. Last and T. M. Alam, *Langmuir*, 2002, **18**, 3714–3721.
74 T. Hayashita, A. Yamauchi, A.-J. Tong, J. C. Lee, B. D. Smith and N. Teramae, *J. Incl. Phenom. Macrocycl. Chem.*, 2004, **50**, 87–94.
75 Y. Nakahara, T. Kida, Y. Nakatsuji and M. Akashi, *J. Org. Chem.*, 2004, **69**, 4403–4411.
76 K. Fujimoto, Y. Muto, M. Inouye, *Chem. Commun.*, 2005, 4780–4782.
77 H. J. Kim, S. H. Kim, D. T. Quang, J. H. Kim, I.-H. Suh and J. S. Kim, *Bull. Korean Chem. Soc.*, 2007, **28**, 811–815.
78 J. Xie, M. Ménand, S. Maisonneuve and R. Métivier, *J. Org. Chem.*, 2007, **72**, 5980–5985.
79 F. M. Jradi, M. H. Al-Sayah and B. R. Kaafarani, *Tetrahedron Lett.*, 2008, **49**, 238–242.

This journal is © The Royal Society of Chemistry 20xx

Please do not adjust margins

80 Y. Nakatsuji, M. Nakamura, T. Oka and M. Muraoka, *Chem. Lett.*, 2011, **40**, 1226–1228.
81 D. Thongkum and T. Tuntulani, *Tetrahedron*, 2011, **67**, 8102–8109.
82 D. Kraskouskaya, M. Bancerz, H. S. Soor, J. E. Gardiner and P. T. Gunning, *J. Am. Chem. Soc.*, 2014, **136**, 1234–1237.
83 Z. Jarolímová, M. Vishe, J. Lacour and E. Bakker, *Chem. Sci.*, 2016, **7**, 525–533.
84 H. Maeda, K. Hirose and M. Segi, *J. Lumin.*, 2018, **204**, 269–277.
85 K. Kubo, N. Kato and T. Sakurai, *Acta Cryst.*, 1997, **C53**, 132–134.
86 N. Kh. Petrov, W. Kühnle, T. Fiebig and H. Staerk, *J. Phys. Chem. A*, 1997, **101**, 7043–7046.
87 J.-Y. Li, M.-L. Peng, L.-P. Zhang, L.-Z. Wu, B.-J. Wang and C.-H. Tung, *J. Photochem. Photobiol. A*, 2002, **150**, 101–108.
88 J.-Y. Li, B. Chen, L.-P. Zhang, L.-Z. Wu and C.-H. Tung, *Res. Chem. Intermed.*, 2002, **28**, 517–526.
89 S. A. Ahmed, M. Tanaka, H. Ando, K. Tawa and K. Kimura, *Tetrahedron*, 2004, **60**, 6029–6036.
90 W. Zhou, S. Zhang, G. Li, Y. Zhao, Z. Shi, H. Liu and Y. Li, *ChemPhysChem*, 2009, **10**, 2066–2072.
91 E. J. Parra, F. X. Rius and P. Blondeau, *Analyst*, 2013, **138**, 2698–2703.
92 H. Nakai, K. Kitagawa, H. Nakamori, T. Tokunaga, T. Matsumoto, K. Nozaki and S. Ogo, *Angew. Chem. Int. Ed.*, 2013, **52**, 8722–8725.
93 B. E. Kucera, R. E. Jilek, W. W. Brennessel and J. E. Ellis, *Acta Cryst.*, 2014, **C70**, 749–753.
94 B. Klepetárová, M. Kvícalová, D. Sykora, E. Makrlík and P. Vanura, *Inorg. Chim. Acta*, 2018, **477**, 165–171.
95 H. Pasalic, A. J. A. Aquino, D. Tunega, G. Haberhauer, M. H. Gerzabek and H. Lischka, *J. Mol. Model.*, 2017, **23**, 131.
96 B. K. Min, S.-S. Lee, S. M. Kang, J. Kim, D. W. Kim and S. Lee, *Bull. Korean Chem. Soc.*, 2018, **39**, 1047–1053.
97 *The Nature of the Chemical Bond*, ed. L. Pauling, Cornell University Press, Ithaca, NY, 3rd en, 1960.
98 H. Kuroda, I. Ikemoto and H. Akamatu, *Bull. Chem. Soc. Jpn.*, 1966, **39**, 547–551.
99 I. Ikemoto and H. Kuroda, *Acta Cryst.*, 1968, **B24**, 383–387.
100 I. Ikemoto and H. Kuroda, *J. Synth. Org. Chem. Jpn.*, 1969, **27**, 493–506.
101 K. H. Grellmann, A. R. Watkins and A. Weller, *J. Phys. Chem.*, 1972, **76**, 3132–3137.
102 H. Kaino and H. Sato, *J. Phys. Soc. Jpn.*, 1978, **44**, 685–686.
103 A. S. Tiwary and A. K. Mukherjee, *Chem. Phys. Lett.*, 2014, **610–611**, 19–22.
104 Y. García-Rodeja and I. Fernández, *J. Org. Chem.*, 2017, **82**, 8157–8164.
105 J. M. G. Martinho, *J. Phys. Chem.*, 1989, **93**, 6687–6692.
106 J. Grimshaw and J. Trocha-Grimshaw, *J. Chem. Soc. Perkin Trans. 1*, 1972, 1622–1623.
107 X. Zhang, H. Wang, S. Wang, Y. Shen, Y. Yang, K. Deng, K. Zhao, Q. Zeng and C. Wang, *J. Phys. Chem. C*, 2013, **117**, 307–312.
108 Y. Niko, S. Sasaki, K. Narushima, D. K. Sharma, M. Vacha and G. Konishi, *J. Org. Chem.*, 2015, **80**, 10794–10805.
109 K. W. Bair, R. L. Tuttle, V. C. Knick, M. Cory and D. D. McKee, *J. Med. Chem.*, 1990, **33**, 2385–2393.
110 P. F. Driscoll, E. F. Douglass, Jr., M. Phewluangdee, E. R. Soto, C. G. F. Cooper, J. C. MacDonald, C. R. Lambert and W. G. McGimpsey, *Langmuir*, 2008, **24**, 5140–5145.
111 T. Sakai, K. Miyata, S. Tsuboi, A. Takeda, M. Utaka and S. Torii, *Bull. Chem. Soc. Jpn.*, 1989, **62**, 3537–3541.
112 T. Otsubo, S. Mizogami, Y. Sakata and S. Misumi, *Mem. Inst. Sci. Ind. Res. Osaka Univ.*, 1970, **27**, 129–133.
113 P.-N. Cheng, C.-F. Lin, Y.-H. Liu, C.-C. Lai, S.-M. Peng and S.-H. Chiu, *Org. Lett.*, 2006, **8**, 435–438.
114 D. Y. Kim, G. M. Jung, Y. H. Cho, H. Y. Choi, Republic of Korea, KR2020090059.
115 S. J. Choi, D. S. Yang, E. S. Lee, H. Y. Choi, Y. H. Cho and D. Y. Kim, World Intellectual Property Organization, WO2019164231.
116 S. Malashikhin and N. S. Finney, *J. Am. Chem. Soc.*, 2008, **130**, 12846–12847.
117 S. Chen, J. Duhamel and M. A. Winnik, *J. Phys. Chem. B*, 2011, **115**, 3289–3302.

This journal is © The Royal Society of Chemistry 20xx

Please do not adjust margins